

# Platoons of connected vehicles can double throughput in urban roads\*

Jennie Lioris, Ramtin Pedarsani, Fatma Yildiz Tascikaraoglu and Pravin Varaiya

## Abstract

Intersections are the bottlenecks of the urban road system because an intersection's capacity is only a fraction of the flows that the roads connecting to the intersection can carry. This capacity can be increased if vehicles can cross the intersections in platoons rather than one by one as they do today. Platoon formation is enabled by connected vehicle technology. This paper assesses the potential mobility benefits of platooning. It argues that saturation flow rates, and hence intersection capacity, can be doubled or tripled by platooning. The argument is supported by the analysis of three queuing models and by the simulation of a road network with 16 intersections and 73 links. The queuing analysis and the simulations reveal that a signalized network with fixed time control will support an increase in demand by a factor of (say) two or three if all saturation flows are increased by the same factor, with no change in the control. Furthermore, despite the increased demand vehicles will experience the same delay and travel time. The same scaling improvement is achieved when the fixed time control is replaced by the max pressure adaptive control. Part of the capacity increase can alternatively be used to reduce queue lengths and the associated queuing delay by decreasing the cycle time. Impediments to the control of connected vehicles to achieve platooning at intersections appear to be small.

## 1 Introduction

Connected vehicle technology (CVT) has aroused interest in the academic community as well as in automobile and IT companies. Researchers are exploring ways to achieve the ambitious information, mobility and safety goals announced by the USDOT ITS Joint Program Office (USDOT (2015)):

Information: "Vehicle-to-infrastructure (V2I) capabilities and anonymous information from passengers' wireless devices relayed through dedicated short-range communications (DSRC) and other wireless transmission media, has the potential to provide transportation agencies with dramatically improved real-time traffic, transit, and parking data, making it easier to manage transportation systems for maximum efficiency and minimum congestion."

Safety: CVT can "increase situational awareness and reduce or eliminate crashes through vehicle-to-vehicle (V2V) and V2I data transmission. V2V and V2I applications enable vehicles to inform drivers of roadway hazards and dangerous situations that they can't see through driver advisories, driver warnings, and vehicle and/or infrastructure controls."

---

\*This research was supported by the California Department of Transportation. We thank Rene Sanchez of Sensys Networks for the data in Figure 2, and Alex A. Kurzhanskiy, Gabriel Gomes, Roberto Horowitz, Sam Coogan and others in the Berkeley Friday Arterial seminar for stimulating discussions.

Mobility: CVT can “identify, develop, and deploy applications that leverage the full potential of connected vehicles, travelers, and infrastructure to enhance current operational practices and transform future surface transportation systems management.”

The most important academic program on CVT has been the Safety Pilot Model Deployment (Bezzina and Sayer (2015)). Its objective was to assess “a real-world deployment of V2V technology,” involving 300 vehicles that could receive and send safety messages (curve speed warning, emergency electronic brake light, and forward collision warning) and 2300 other vehicles, equipped with communications-only devices with no safety applications, serving as ‘target’ vehicles. The pilot demonstrated the capability to exchange messages using DSRC equipment from different suppliers. The NHTSA report (Harding et al. (2014)) describes the enhanced safety that V2V communications potentially offers in many pre-crash scenarios. Yoshida (2014) gives a readable account of the report’s highlights.

Considerable research effort has been devoted to the formation and performance of wireless vehicular ad-hoc networks (VANETs) in a mobile environment. There also is research on vehicle control using V2V communication to perform maneuvers such as cooperative adaptive cruise control (CACC), merging and safe passage through an intersection (Ploeg et al. (2011); Kianfar et al. (2012); Milanese et al. (2014); Wolterink et al.; Hafner et al. (2013); Au et al. (2015)). This research indicates the potential for automating some driving tasks, with possible side benefits in terms of mobility and safety.

Commercial effort in CVT seeks to stimulate and meet consumer demand to connect their cars to the internet: operate your cellphone, send a message or play a specific song hands-free, and remotely monitor if your car is exceeding a preset speed. These commercial efforts are not primarily intended to promote mobility or safety. Driver assistance technologies, including ACC, lane-departure warning and self-driving cars, do seek to enhance safety, but they are vehicle-resident technologies that do not rely on V2V communication. Neither academic nor commercial research is concerned with enhancing mobility.

This paper explores the use of CVT to directly increase the capacity of urban roads based on the simple idea that if CVT can enable organizing vehicles into platoons, the capacity of an intersection can be increased by a factor of two to three. §2 sketches a scenario showing how platooning increases an intersection’s capacity. The capacity increase will make it possible to support an increase in demand in the same proportion, with no change in the signal control. Alternatively, some of the capacity increase can be used to reduce queues and the associated delay at intersections. An argument for this ‘free’ capacity increase is based on an analysis of three queuing models in §3 that predict the mobility benefits of platooning. The simulation exercise in §4 lends plausibility to those predictions. §5 summarizes the main conclusions of this study.

## 2 Intersection capacity

The Highway Capacity Manual (Transportation Research Board (2010)) defines an intersection’s capacity as

$$\text{Capacity} = \sum_i s_i \frac{g_i}{T}, \quad (1)$$

in which  $T$  is the cycle time and, for lane group  $i$ ,  $s_i$  is the saturation flow rate and  $g_i/T$  is the effective green ratio. HCM takes  $s_i = N \times s_0 \times f$ :  $N$  is the number of lanes in the group,  $s_0$  is the base rate in vehicles per hour (vph), and  $f$  is an ‘adjustment factor’ that depends on the road geometry and nature of the traffic. The base rate  $s_0$  is obtained from a thought experiment: it is the maximum discharge rate from an infinitely long queue of vehicles facing a permanently green signal. HCM recommends  $s_0 = 1,900$  vph. Note that  $s_i \times (g_i/T)$  is the rate at which vehicles in queue in group  $i$  can potentially be served by the intersection. So we also call it the *service rate* in a queuing model of this lane group.

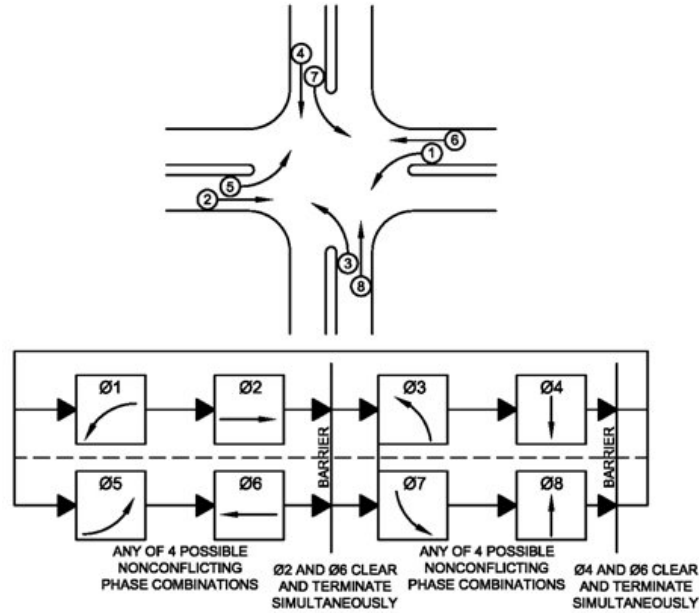


Figure 1: An intersection with four approaches, each with a through and left-turn movement (top), and a ring-and-barrier diagram to organize the movements (bottom). Source: FHWA.

Consider an intersection with four approaches, each with one through lane and one left-turn lane as in Figure 1 (top). There are thus eight movements in all. Suppose each lane supports a flow up to 1,900 vph for a total of  $1,900 \times 8 = 15,200$  vph. However, from Figure 1 (bottom) only two movements can safely be actuated at the same time, so the effective green ratio for each movement is at most 0.25, and from equation (1) the capacity of the intersection is only 3,800 vph. Thus the intersection is the principal bottleneck in urban roads: its capacity is a fraction (here 1/4) of the capacity of the roads connecting to it.

Figure 2 (left) is a schematic of the system of vehicle detectors installed at an intersection in Santa Clarita, CA. Each tiny white dot is a magnetic sensor that reports the times at which a vehicle enters and leaves its detection zone. When there is a pair of detectors, like at every stop bar and some advanced locations, the speed of the vehicle is also estimated and reported. The detection system also receives the signal phase timing from the conflict monitor card in the controller cabinet (not shown in the figure). These measurements

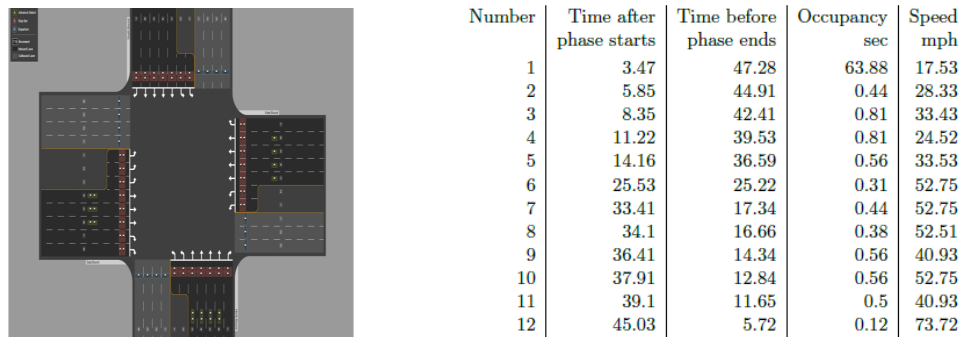


Figure 2: Schematic of intersection detection system (left), a trace of vehicles entering intersection from one through lane during one green phase (right).

can be processed to obtain all intersection performance measures, including V/C (volume to capacity) ratios, fraction of arrivals in green, as well as red-light violations (Day et al. (2014)). From the times at which each vehicle enters the intersection we get the empirical saturation flow rate, that is the rate at which vehicles actually move through the intersection during the green phase, and the vehicle headway.

Figure 2 (right) displays the trace of 12 vehicles that enter a through lane in the intersection during one cycle with a green phase duration of 50 sec for the through movement. The second and third columns give the times (in sec) after the start of green and before the end of green that each vehicle enters the intersection, the fourth column gives the duration of time the vehicle ‘occupied’ the detector zone, and the fifth column lists an estimate of its speed. The detectors have a sampling frequency of 16 Hz, so the speeds are quantized (the distance between the two detectors is 12 feet), and speeds above 60 mph have a quantization error of about 15 mph, speeds below 30 mph have an error under 5 mph. The average speed of the 12 vehicles is 42 mph. The speed limit at this intersection is 50 mph. The first vehicle entering the intersection has a delay or reaction time of 3.47 sec. The first 5 vehicles enter within 14.16 sec, so the empirical saturation flow rate of this movement is  $14.16/5 = 2.83$  sec per veh or  $3600/2.83 = 1272$  veh/hour. Vehicles 5, 6, ... travel at much higher speed.

Suppose these 12 vehicles were all to move as a platoon, that is, at the same speed of 45 mph (66 feet/sec) with a uniformly small time headway of (say) 0.75 s (the space headway would be  $0.75 \times 66 = 49.5$  ft), giving a saturation flow rate of  $3600/0.75 = 4800$  vph, which is 3.8 times the observed rate of 1272 vph and 2.5 times HCM’s theoretical rate of 1900 vph. (Note that the headway between vehicles 7 and 8 in Figure 2 (right) is 0.7 sec.) An estimate for an intersection with speed of 30 mph (44 feet/sec) and a space headway of 40 feet is a platoon saturation flow rate of  $(40/44) \times 3600 = 3960$  vph, which is twice HCM’s 1900 vph and up to three times the rates observed in today’s intersections.

What does it take to organize a platoon? If the 12 vehicles queued at (or approaching) the intersection in Figure 2 were ‘connected’ that is, if they were to communicate with each other as well as with the signal controller, their longitudinal motion could be controlled in such a way that they would move together as a platoon and thereby increase the saturation flow rate by two or three. Platooning seems quite feasible given that autonomous platoons (of vehicles with 16 ft headway at 60 mph) were demonstrated 20 years ago in 1997 by the National Automated Highway System Consortium (NAHSRC; Shladover (2013)). Since then vehicle automation has been greatly facilitated by advances in actuation (electronic braking, throttle and steering) and sensing (radar and lidar), while platoon stability and control design are much better understood.

Indeed, Ploeg et al. (2011) report an experiment of a 6-vehicle CACC platoon, with a 0.5s headway. The ACC equipped vehicles were augmented with V2V communications using a 802.11a WiFi radio in ad-hoc mode. Milanés et al. (2014) describe experiments with a 4-vehicle platoon, capable of cut-in, cut-out and other maneuvers, using CACC technology. The vehicles had factory-equipped ACC and their capability was enhanced by a DSRC radio that permitted V2V communication needed to enable CACC. The vehicles in the platoon had a time gap of 0.6 sec (time headway of 0.8 s) traveling at 55 mph.

Of course challenges in control and communication will be encountered and must be overcome, if the idea proposed here is to be realized. In that sense the paper is a ‘forward looking statement’: it assumes that vehicles can be organized as platoons when they cross an intersection and explores what throughput and delay advantages such organization can bring.

It is important to distinguish our proposal to use CACC to increase an intersection’s capacity from proposals to use CACC to increase highway capacity by decreasing headway. Increasing the throughput of urban roads will *not* increase the throughput of the urban network which is limited by intersection capacity.

### 3 Three predictions

Suppose magically that all saturation flow rates in an urban road network of signalized intersections are increased by the same factor of 2 to 3 using platoons. It seems obvious that this change will increase throughput and reduce travel time. It is less clear how much the improvement would be, since the links at an intersection may get filled up by vehicles arriving more rapidly than at the normal rate, and thereby block additional arrivals.

An exact analysis of the stochastic queuing network that models the road network is beyond our reach. So we use three models to predict the average queue size and delay of vehicles, and throughput, beginning with the simplest model for an isolated intersection, namely the M/M/1 queue. We will see that the predictions from the M/M/1 queue are unduly optimistic because its service process does not reflect the stop-go nature of signal lights.

For the second model we propose a memoryless queue with an on/off (green/red) service process that better models signal actuation. We use the Recursive Renewal Reward (RRR) technique to exactly analyze the Markov chain corresponding to this queue, and characterize the behavior of the system as both arrival and saturation rates increase proportionately. The predictions of this second model are more reasonable.

Lastly we investigate the behavior of the fluid queuing network proposed in Muralidharan et al. (2015), as saturation flows and arrival rates are increased. We show consistency between the predictions of the second model and the fluid network model. We develop an example to indicate the challenges in dealing with finite capacity queues.

#### 3.1 Model 1: M/M/1 queue

Consider an M/M/1 queue with arrival rate  $\lambda$  and service rate  $\mu$  as the model of the queue at a single approach of an isolated intersection. Vehicles arrive at this approach at rate  $\lambda$  vph and are served at rate  $\mu$  vph, the saturation flow rate multiplied by the effective green ratio of the approach (see (1)).

As is known the stability region of the system is  $\lambda < \mu$ , and the average delay or time spent in the queue by a vehicle is  $\frac{1}{\mu} \times \frac{\rho}{1-\rho}$ , where  $\rho = \lambda/\mu$  is the load of the system ( $\rho$  is also the ‘volume-capacity or VC ratio’). Now if  $\mu$  is increased to  $C\mu$  for  $C > 1$ , the stability region is increased  $C$ -fold to  $\lambda < C\mu$ . Further, if the demand is also increased to  $C\lambda$ , the average delay of the system is *decreased* by a factor  $C$  since the load  $\rho$  is unchanged. This suggests that increasing the saturation flow rates by a factor  $C$  leads to an increase in throughput and a decrease in delay by the same factor  $C$ . This double benefit is too good to be true.

One immediate objection to the ‘double benefit’ is that the queues at an intersection have finite capacity so it is more appropriate to consider the M/M/1/ $K$  queue, where  $K$  is the finite capacity of the queue. Again for  $\rho = \frac{\lambda}{\mu}$  the stationary distribution of the length of the M/M/1/ $K$  queue is

$$\pi_k = \frac{\rho^k}{\sum_{i=0}^K \rho^i} = \rho^k \frac{1-\rho}{1-\rho^{K+1}}, \quad k = 0, 1, \dots, K, \quad (2)$$

in which  $\pi_k$  is the probability that there are  $k$  vehicles in queue. New arrivals are blocked when the queue is full, which occurs with probability  $\pi_K$ ; thus, the effective throughput of the system is  $\lambda_e = \lambda(1 - \pi_K)$ . The expected queue length is

$$\bar{N} = \sum_{k=0}^K k\pi_k = \frac{\rho(1 - (K+1)\rho^K + K\rho^{K+1})}{(1-\rho)(1-\rho^{K+1})}, \quad (3)$$

and the average delay by Little's law is  $\bar{D} = \frac{\bar{N}}{\lambda_e}$ .

As one can see from the formulas, the blocking probability  $\pi_K$  and hence the throughput depends only on  $\rho$ . Thus if  $\mu$  and  $\lambda$  are increased by the same factor  $C$ , the blocking probability  $\pi_K$  is unchanged. Hence the throughput will be increased by  $C$ , since  $\lambda_e = \lambda(1 - \pi_K)$ , while the delay will be decreased by a factor  $C$ . (The blocking probability is small for reasonable parameters: with  $\rho$  or VC ratio equal to 0.8 and  $K = 10$ , the blocking probability is 0.02.) Thus the double benefit of the M/M/1 model is assured even with finite capacity links.

The M/M/1/ $K$  Model confirms one intuition: if the saturation flow of all links along an arterial is increased by factor  $C$ , it is the shortest link (smallest  $K$ ) that will limit the increase in throughput. But this intuition may be too simplistic in ignoring the possibility of designing offsets so that platoons travel in a green wave unhindered by the small capacity of short links rather than in the Poisson stream of the M/M/1/ $K$  model. However, the main reason the M/M/1/ $K$  model is unduly optimistic is that it replaces the on-off (green-red) nature of signal actuation by a constant saturation rate. The next model does not have this defect.

### 3.2 Model 2: Single queue with on/off memoryless service

Consider a single queue with on/off service: it receives full service when the light is green and no service when the light is red. The queue behavior is modeled as the Markov chain of Figure 3:  $(x, g)$  is the state when there is full service (the light is green) and the queue length is  $x$ , and  $(x, r)$  is the state with no service (the light is red) and the queue length is  $x$ . We consider a Poisson clock model for the state transitions, so time is continuous and the labels are transition rates. We show that like in the M/M/1 model there is a throughput benefit but unlike in that model there is no delay benefit when the demand and service rates both are increased by  $C$ .

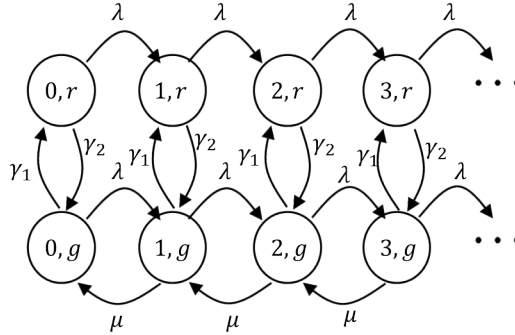


Figure 3: Markov chain of a memoryless queue with on/off service.

We compute the average delay corresponding to the Markov chain in Figure 3 using the *Recursive Renewal Reward* (RRR) technique described by Gandhi et al. (2013). RRR is based on renewal reward theory and busy period analysis of a 2-dimensional Markov chain like the one in Figure 3 that is finite in one of the dimensions. This Markov chain can also be analyzed by matrix-analytic methods (Latouche and Ramaswami (1999)), but the RRR technique is better as it does not require computing the stationary distribution of the chain to determine the average delay (or other metrics).

First note that the chain is in a green state for the fraction  $\frac{\gamma_2}{\gamma_1 + \gamma_2}$  of the time on average, so in accordance with (1) the effective service rate is  $\frac{\gamma_2}{\gamma_1 + \gamma_2} \mu$  and the chain is stable if  $\lambda < \frac{\gamma_2}{\gamma_1 + \gamma_2} \mu$ . We define a renewal cycle as the process that starts from state  $(0, g)$  and returns back to this state for the first time. Imagine that the

process collects a reward in each state  $(x, y)$  equal to the number  $x$  of vehicles in the queue ( $y = g, r$ ). Let  $R$  be the expected reward in a cycle, and let  $T$  be the expected duration of a cycle. Then the average number of vehicles in the queue is  $R/T$ , so the average delay is  $\frac{R}{\lambda T}$ . We use the birth-death property of the Markov chain to find linear recursive equations to calculate  $R$  and  $T$  as follows. Let  $T_{x,g}^L$  be the expected time to visit state  $(x-1, g)$  from state  $(x, g)$  (expected time to go one level left), and let  $T_{x,r}^L$  be the expected time to visit state  $(x, g)$  from state  $(x, r)$ . Let  $R_{x,g}^L$  be the expected reward collected starting from state  $(x, g)$  to state  $(x-1, g)$ , and let  $R_{x,r}^L$  be the expected reward accumulated starting from state  $(x, g)$  to state  $(x, r)$ . We then have the following linear relations:

$$T = \frac{1}{\lambda + \gamma_1} + \frac{\lambda}{\lambda + \gamma_1} T_{1,g}^L + \frac{\gamma_1}{\lambda + \gamma_1} T_{0,r}^L, \quad (4)$$

$$T_{1,g}^L = \frac{1}{\lambda + \mu + \gamma_1} + \frac{\lambda}{\lambda + \mu + \gamma_1} (T_{1,g}^L + T_{2,g}^L) + \frac{\gamma_1}{\lambda + \mu + \gamma_1} (T_{1,r}^L + T_{1,g}^L), \quad (5)$$

$$T_{0,r}^L = \frac{1}{\lambda + \gamma_2} + \frac{\lambda}{\lambda + \gamma_2} (T_{1,r}^L + T_{1,g}^L). \quad (6)$$

By the repetitive structure of the Markov chain, we have  $T_{1,r}^L = T_{0,r}^L$  and  $T_{2,g}^L = T_{1,g}^L$ . Thus, one can solve these three linear equations to find the three variables  $T$ ,  $T_{1,g}^L$  and  $T_{0,r}^L$ . One can similarly write linear relations for the reward:

$$R = \frac{0}{\lambda + \gamma_1} + \frac{\lambda}{\lambda + \gamma_1} R_{1,g}^L + \frac{\gamma_1}{\lambda + \gamma_1} R_{0,r}^L, \quad (7)$$

$$R_{1,g}^L = \frac{1}{\lambda + \mu + \gamma_1} + \frac{\lambda}{\lambda + \mu + \gamma_1} (R_{1,g}^L + R_{2,g}^L) + \frac{\gamma_1}{\lambda + \mu + \gamma_1} (R_{1,r}^L + R_{1,g}^L), \quad (8)$$

$$R_{0,r}^L = \frac{0}{\lambda + \gamma_2} + \frac{\lambda}{\lambda + \gamma_2} (R_{1,r}^L + R_{1,g}^L). \quad (9)$$

By Theorem 2 of Gandhi et al. (2013), since the reward at each state is the number of vehicles in the queue,  $R_{2,g}^L = R_{1,g}^L + T_{1,g}^L$  and  $R_{1,r}^L = R_{0,r}^L + T_{0,r}^L$ . Solving these equations one finds  $R$ ,  $R_{1,g}^L$ , and  $R_{0,r}^L$ . The average queue length is

$$\bar{N} = \frac{R}{T} = \frac{\lambda \gamma_1^2 + 2\lambda \gamma_1 \gamma_2 + \lambda \gamma_1 \mu + \lambda \gamma_2^2}{(\gamma_1 + \gamma_2)(\gamma_2 \mu - \lambda(\gamma_1 + \gamma_2))}. \quad (10)$$

As a check, observe that when  $\gamma_1 = 0$ , the expression reduces to  $\lambda/(\mu - \lambda)$ , the same as for the M/M/1 queue, as expected. Further, when  $\lambda$  approaches the capacity limit  $\frac{\gamma_2}{\gamma_1 + \gamma_2} \mu$ , the expected number of vehicles in the queue tends to infinity. By Little's law, the average delay is

$$\bar{D} = \frac{\bar{N}}{\lambda} = \frac{\gamma_1 + \gamma_2 + \frac{\gamma_1}{\gamma_2 + \gamma_1} \mu}{\gamma_2 \mu - \lambda(\gamma_1 + \gamma_2)}. \quad (11)$$

We study how the delay and queue length change as both demand and service rates and cycle times are scaled. To focus ideas, take the base case to be  $\mu^0 = 2000$  vph,  $\lambda^0 = 900$  vph,  $\gamma_1^0 = \gamma_2^0 = \gamma^0 = 30$  switches per hour, corresponding to 30 cycles per hour or a cycle time of 120 sec and an effective green ratio of 0.5. We scale these parameters as  $\mu = C\mu^0$ ,  $\lambda = C\lambda^0$ ,  $\gamma_1 = \gamma_2 = g\gamma^0$ . Substituting these values into (11) gives

$$\bar{D} = \frac{1}{g} \frac{60g + 1000C}{30 \times 200C}, \quad \bar{N} = C\lambda^0 \times \bar{D}. \quad (12)$$

For  $g = 1$  (no change in cycle time) we see that the average delay  $\bar{D}$  does not materially change as  $C$  is increased to 2 or 3, while the average number  $\bar{N}$  increases linearly with  $C$ . Thus this on-off model suggests

two predictions as the saturation flow rate increases by a factor  $C$ : (1) the network can support a demand that increases by the same factor, (2) the queue ( $\bar{N}$ ) grows by the same factor, but the queuing delay ( $\bar{D}$ ) is unchanged.

Another prediction can be extracted by considering the effect of an increase in  $g$ , which decreases the cycle time by the factor  $g$ , while keeping the effective green ratios the same. We see from expression (12) that the average delay  $\bar{D}$  and the queue size  $\bar{N}$  decrease almost linearly with  $g$ . This gives a third prediction: (3) the queue length can be or reduced by reducing the cycle time.

### 3.3 Model 3: Fluid model of queuing network

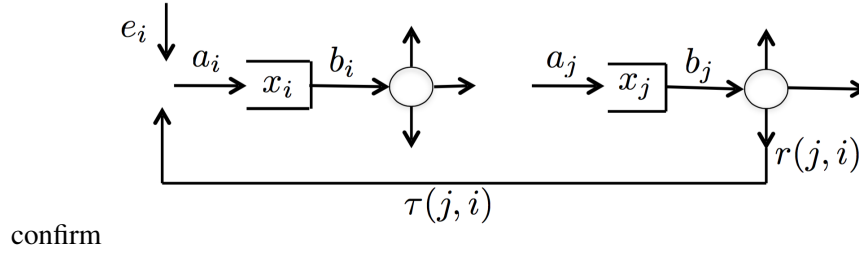


Figure 4: Network of fluid model. Source: Muralidharan et al. (2015).

We now analyze a fluid model of a network of signalized intersections, all with fixed-time control with the same cycle time  $T$ . The model was studied by Muralidharan et al. (2015) and illustrated in Figure 4. There are  $J$  queues in the network, each corresponding to one turn movement. A specified fraction  $r(j, i)$  of the vehicles departing from queue  $j$  is routed to queue  $i$ . Queue  $i$  also has exogenous arrivals with rate  $e_i(t)$ . The exogenously specified service rate of queue  $i$ ,  $c_i(t)$ , is periodic with period  $T$ :  $c_i(t)$  is the saturation flow rate when the light is green and  $c_i(t) = 0$ , when it is red.  $x_i(t)$  is the queue length of  $i$  and  $b_i(t)$  is its departure rate at time  $t$ .  $a_i(t)$  denotes the total arrival rate into queue  $i$  at time  $t$ . The travel time from queue  $j$  to queue  $i$  on link  $(j, i)$  is  $\tau(j, i)$  as in the figure. The network dynamics are as follows.

$$\dot{x}_i(t) = a_i(t) - b_i(t), \quad (13)$$

$$a_i(t) = e_i(t) + \sum_{j=1}^J b_j(t - \tau(j, i))r(j, i), \quad (14)$$

$$b_i(t) = \begin{cases} c_i(t), & \text{if } x_i(t) > 0, \\ \in [0, c_i(t)], & \text{if } x_i(t) = 0, \\ 0, & \text{if } x_i(t) < 0. \end{cases} \quad (15)$$

This is a nonlinear differential inclusion with delay: nonlinear because  $b_i(t)$  is nonlinear in  $x_i(t)$ , inclusion (rather than equation) because the right-hand side of (15) is set-valued, and the  $\tau(j, i)$  introduce delay. The inclusion is not Lipschitz, but Muralidharan et al. (2015) show that (13)-(15) has a unique solution for  $x_i(0) \geq 0$ . The exogenous parameters of the system are the rates  $\{e_i(t), c_i(t)\}$  and the initial state  $x(0)$ .

The system (13)-(15) is positively homogeneous of degree one. That is, if  $\{x(t), a(t), b(t)\}$  is the solution for a specified  $\{x(0), e(t), c(t)\}$  and  $C > 0$ , then  $\{Cx(t), Ca(t), Cb(t)\}$  is the solution for  $\{Cx(0), Ce(t), Cc(t)\}$ . Hence if the exogenous arrivals  $e$  and the saturation flow rate are both increased by a factor  $C$ , the queue  $x(t)$  and the departures  $b(t)$  both increase by the same factor. Thus the model predicts the first benefit of higher service rate (by platooning), namely, throughput increase.



What about queue length and delay? The average queue length at  $i$  over (say) one cycle beginning at time  $t_0$  in the base case ( $C = 1$ ) is

$$\bar{x}_i(t_0) = \frac{1}{T} \int_{t_0}^{t_0+T} x_i(t) dt,$$

and if the service and arrival rates (and the initial queue  $x(0)$ ) are increased by a factor  $C$ , the average queue length over the same cycle also increases by the same factor:

$$\frac{1}{T} \int_{t_0}^{t_0+T} Cx_i(t) dt = C\bar{x}_i(t_0). \quad (16)$$

Since the queue length, arrival and departure processes all increase by the same factor, it is immediate that the average delay per vehicle in each queue is *unchanged*. Since the travel time is the sum of the queuing delays and the free flow travel time along a route, and both of these are unchanged by the scale factor  $C$ , it follows that the travel time is unchanged as well. This result does not even require the system to be stable, i.e. queues to be bounded.

In summary, the on-off queue (Model 2) and the fluid network (Model 3) yield a consistent prediction: If the saturation flow for every movement is increased by a factor  $C$ , the network can support a throughput that increases by  $C$ , while keeping the queuing delay and travel time unchanged.

### 3.4 Queues with finite capacity: An example

In all three models above, the queue capacity is taken to be infinite. Since the queues in the second and third models grow in proportion to the scale factor  $C$  of the saturation rates, the link may become saturated, and the throughput gain may be less than  $C$ . We illustrate this in a simple example using the fluid model. Rigorous analysis of the queuing network with finite capacity queues appears to be a difficult problem.

Consider a single queue with capacity of 20 vehicles, so arrivals are blocked once the queue length reaches 20. Consider a constant arrival rate,  $e(t) = a(t) = 10$ , and the following service rate in one period  $T = 2$ :

$$c(t) = \begin{cases} 0, & t \in [0, 1) \\ 30, & t \in [1, 2) \end{cases}.$$

Then  $\bar{c} = 15 > \bar{a} = 10$ , so the queue is stable. If  $x(0) = 0$ , the trajectory is periodic with period  $T$  and easily calculated to be

$$x(t) = \begin{cases} 10t, & t \in [0, 1) \\ \max(30 - 20t, 0), & t \in [1, 2) \end{cases}.$$

The maximum queue-length occurs at the end of red, at  $t = 1 + nT$ ,  $n = 0, 1, \dots$ , and equals  $x(1) = 10$ .

Now suppose that the saturation flow rate and the arrival rate are increased by a factor of 3. Then  $\bar{c} = 3 \times 15 = 45$  will also be the maximum throughput of the system in the case of infinite capacity, and the queue will increase by a factor of 3, so the maximum queue length will be 30. This is larger than the 20 vehicle limit for the finite capacity queue. If the arrival rate is  $a(t) = 3 \times 10 = 30$ , the queue will be blocked during the interval  $t \in [2/3, 1]$ . The maximum throughput of the finite-capacity queue is easily calculated to be  $\frac{20+30}{2} = 25 = 5/9 \times 45$ , which is only 55 percent of the throughput of the infinite-capacity queue.

The storage capacity of the link rather than the intersection has now become the bottleneck, so the throughput gain is reduced to a sub-linear function of the gain  $C$  in the saturation flow rates. Note, however, that in a

network context, whether a link becomes a bottleneck is difficult to determine since it depends on the signal control and the offsets.

**Remark** Suppose the cycle length is decreased to  $T = 2/3$  and the green ratio is unchanged while the saturation flow rate is increased by 3. Then the throughput will still increase by 3, as no blocking of the queue occurs. This is an instance of prediction (3): queues are reduced if the cycle length is reduced, while keeping the green ratios (the  $g_i/T$ ) in (1) the same. The prediction will be validated in the simulations of the next section. There is another moral: if the cycle length is reduced more and more, the M/M/1 model becomes a better fit and the second benefit of lower delay begins to appear.

### 3.5 Reducing cycle time, queue length and delay

We formalize the intuition in the previous example. In the model (13)-(15) change the service rate to  $c(gt)$ , where  $g > 1$ . This means that the cycle time is reduced by  $g$ , but the green ratios are unchanged. Let  $z(t) = g^{-1}x(gt)$ . Then

$$\begin{aligned} \dot{z}_i(t) &= \dot{x}_i(gt) = a_i(gt) - b_i(gt), \\ b_i(gt) &= \begin{cases} c_i(gt), & \text{if } x_i(gt) > 0 \leftrightarrow z_i(t) > 0, \\ \in [0, c_i(gt)(t)], & \text{if } x_i(gt) = 0 \leftrightarrow z_i(t) = 0, \\ 0, & \text{if } x_i(gt) < 0 \leftrightarrow z_i(t) < 0. \end{cases} \end{aligned}$$

Furthermore from (14)

$$a_i(gt) = e_i(gt) + \sum_{j=1}^J b_i(gt - \tau(j, i))r(j, i).$$

Hence

$$z(t) = g^{-1}x(gt) \tag{17}$$

is the queue for exogenous arrivals  $e(gt)$ , and service  $c(gt)$ . Thus by speeding up the service rate by factor of  $g$ , the queue length is reduced by the same factor  $g$ . This is the third prediction.

The third prediction is of a different character, since it has nothing directly to do with increasing saturation flow rate. However, in practice reducing cycle time is not possible because it will lead to a reduction in intersection capacity (the constant lost time due to the yellow and all-red clearance intervals reduces the effective green ratio in (1)), and the base case demand may not be accommodated. But if platooning gives a gain of  $C$  in the saturation flow rate, some of the gain may be used to reduce cycle time, queue length and delay.

## 4 Case study

We now present a simulation study of a road network near Los Angeles, using a mesoscopic simulator called PointQ. The simulator and the network are described in Tascikaraoglu et al. (2015), which reports the base case with exogenous demands at the input links, modeled as stationary Poisson streams, and intersections regulated by fixed time (FT) controls and offsets. PointQ is a discrete event simulation; it accurately models vehicle arrivals, departures and signal actuation. It models queues as ‘vertical’ or ‘point’ queues that discharge at the saturation flow rate when the signal is green, and are fed by exogenous arrivals or by vehicles

that are routed from other queues. When a vehicle is discharged from one queue it travels to a randomly assigned destination queue according to the probability distribution specified by the routing matrix  $\{r(i, j)\}$  (see (14)). The vehicle takes a pre-specified fixed time to travel along the link determined by the assigned destination and then joins the destination queue. Every event in the simulation is recorded and uploaded into a database from which the reported performance measures are calculated.

Figure 5 shows a map of the study site and its representation as a directed graph with 16 signalized intersections, 73 links, and 106 turn movements, hence 106 queues. Each queue corresponds to a movement, so it is convenient to index a queue by a pair  $(m, n)$  in which  $m$  ( $n$ ) is the incoming (outgoing) link index. For example, referring to Figure 5,  $x(139, 104)$  is the number of vehicles in link 139 that are queued up at intersection 103 waiting to go to link 104.

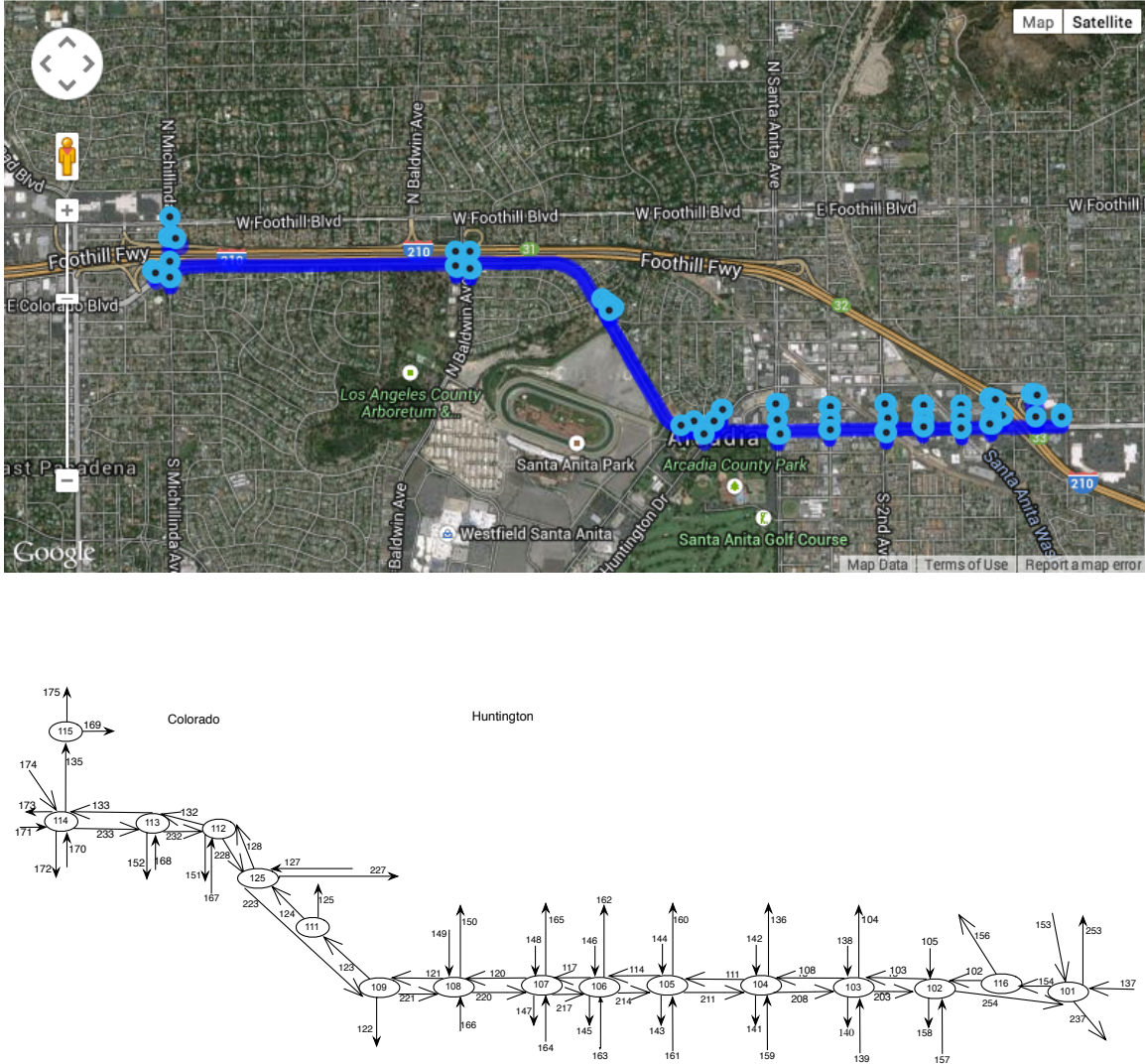


Figure 5: Map of site and corresponding network graph.

For the first set of experiments we increase all the saturated flow rates and the demands by the same factor  $C = 1.0, 1.5, 2.0, 2.5$ , and  $3.0$ , with  $C = 1.0$  being the base case. For the second set of experiments we replace the fixed-time control by the max pressure (MP) adaptive control under two switching regimes: MP4 permits four phase changes per cycle just like for FT control, while MP6 permits six phase changes.

For each experiment we present mean values of queue lengths and queuing delay. Each stochastic simulation lasts 3 hours or 10,800 sec. Since we want to calculate the mean values of queue lengths and delays, and since the queue length process is positive recurrent, it is reasonable to assume that the time average of these quantities over a three-hour long sample path will be close to their statistical mean. Hence the mean values reported below are the empirical time averages. The results confirm all three predictions.

**Queue lengths** Figure 6 shows plots of the sum of all queues for three controls: FT (fixed

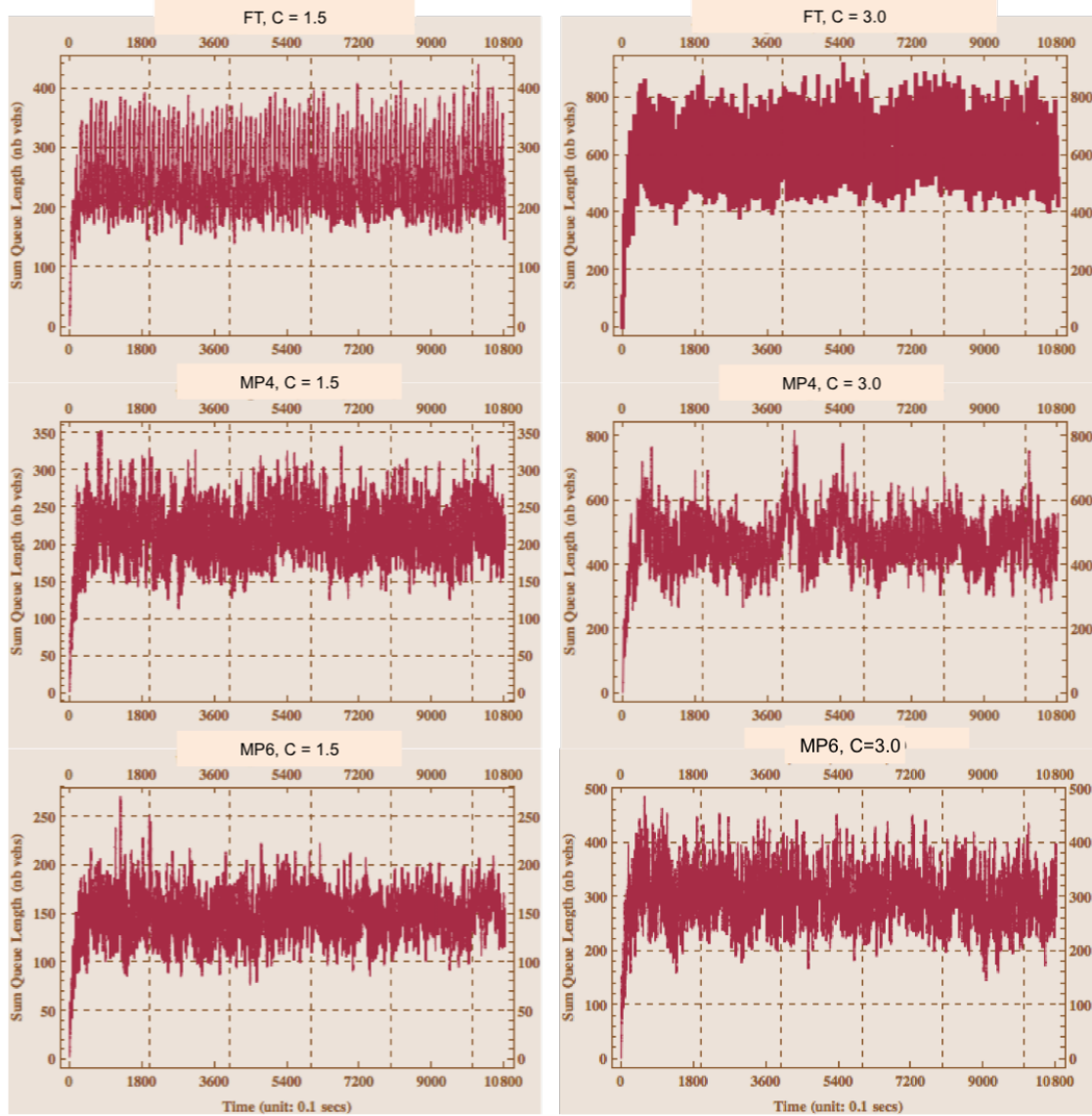


Figure 6: Sum of all queues for FT, MP4, MP6 control when demand and saturation flows are scaled by  $C = 1.5$  and  $3.0$ .

time), MP4 (4 switches per cycle) and MP6 (6 switches per cycle) when the demand and saturation flow rates for the base case are scaled by  $C = 1.5$  and  $3$ . Notice that the queue lengths for  $C = 3$  are approximately twice as large as for  $C = 1.5$ , for all three signal control schemes, as predicted by (16).

Table 1 reports the average sum of all queue lengths. The first column gives the scale factor  $C$  and the average total exogenous demand in vph, e.g. the first column entry in the first row, (1.0, 14,350), refers to

$C$ , Total vph	Signal Control Type	Mean Sum all queues (veh)	Ratio of sum to $C = 1$
1.0, 14350	FT	197.4	1
1.0, 14350	MP4	146.5	1
1.0, 14350	MP6	101.9	1
1.5, 21455	FT	248.6	1.26
1.5, 21455	MP4	213.7	1.49
1.5, 21455	MP6	146.8	1.46
2.0, 28540	FT	347.0	1.76
2.0, 28540	MP4	301.1	2.1
2.0, 28540	MP6	201.1	1.99
2.5, 35950	FT	455.7	2.31
2.5, 35950	MP4	395.0	2.7
2.5, 35950	MP6	248.7	2.46
3.0, 43298	FT	586.2	2.97
3.0, 43298	MP4	470.0	3.2
3.0, 43298	MP6	298.3	2.95

Table 1: Mean total queue length for different demands and signal control.

the base case  $C = 1$  with an exogenous demand of 14,350 vph. The second column indicates the signal control strategy used: FT is fixed time, MP4 is max pressure with 4 changes per cycle, and MP6 is max pressure with 6 changes per cycle. The third column is the average number of vehicles summed over all 106 queues. The fourth column is the ratio of the sum of queue lengths to the sum for the base case,  $C = 1$ . As is seen in the fourth column, this ratio is roughly equal to the scale factor,  $C$ . For example for FT, the sum of queue lengths grows in the proportion 1: 1.26: 1.76: 2.31: 2.97 as the scale increases in the proportion 1: 1.5: 2.0: 2.5: 3.0. This is in conformity with the first two predictions. First, the queue sums are staying bounded, so the increase in the saturation flows by  $C$  does support demands that increase in the same proportion, and the queue lengths grow in the same proportion.

**Queue delay** We now consider queuing delay. The prediction is that the mean queuing delay experienced by a vehicle stays the same despite the increase in demand. Since there are 106 queues in all, we narrow our focus to the six queues at intersection 103. Table 2 gives the delays of each queue as a function of five values of the scale factor  $C$  and three different signal control: FT, MP4 and MP6. Consider for example the queue  $x(138, 140)$ . As the saturation flow rates and the demand increase in proportion 1: 1.5: 2.0: 2.5: 3.0, the mean delay (sec) in this queue under FT changes within a narrow range 22.35: 17.50: 18.99: 19.95: 20.69, while under MP4 the delay varies within the range [10.12, 11.30] and under MP6 the range is [6.73, 7.3]. When the delay is averaged over all queues at intersection 103, the variation with changes in demand is even smaller as is seen in Table 3. Note that three queues at intersection 103 correspond to right turn (RT) movements. Since right turns on red are permitted the impact of increased rates of demand and saturation flow may not be adequately captured by the three models. For this reason, Table 3 reports delays with and without including RT queues.

**Faster phase switching** We now come to the third prediction: queue lengths will decline as the number of phase switches per cycle increases. This is borne out when we compare the sum of queue lengths for MP4 vs MP6, for each level of demand. MP4 permits four and MP6 permits 6 switches per cycle. As Table 1 shows, the queues for MP6 are indeed smaller than for MP4.

In fact the second and third models suggest a quantitative prediction. In (12) and (17)  $g$  is the switching

<i>C</i>	RT	Queue (Movement)	Delay (sec) FT	Delay (sec) MP4	Delay (sec) MP6
1.0	RT	$x(103,104)$	5.82	3.60	2.91
1.0	-	$x(103,108)$	3.07	13.60	8.94
1.0	RT	$x(138,108)$	3.76	3.48	3.28
1.0	-	$x(138,140)$	22.35	11.30	7.30
1.0	RT	$x(139,203)$	2.48	2.42	2.33
1.0	-	$x(139,104)$	21.62	11.17	7.49
1.5	RT	$x(103,104)$	4.22	3.41	2.46
1.5	-	$x(103,108)$	2.36	13.70	7.14
1.5	RT	$x(138,108)$	0.80	2.34	2.31
1.5	-	$x(138,140)$	17.50	10.71	6.76
1.5	RT	$x(139,203)$	0.73	1.57	1.56
1.5	-	$x(139,104)$	18.04	10.72	6.77
2.0	RT	$x(103,104)$	5.08	3.19	2.27
2.0	-	$x(103,108)$	2.30	14.28	6.84
2.0	RT	$x(138,108)$	0.88	1.99	1.93
2.0	-	$x(138,140)$	18.99	10.78	7.20
2.0	RT	$x(139,203)$	0.75	1.25	1.25
2.0	-	$x(139,104)$	19.1	11.09	7.16
2.5	RT	$x(103,104)$	5.67	3.48	2.28
2.5	-	$x(103,108)$	2.19	14.91	6.77
2.5	RT	$x(138,108)$	0.94	1.48	1.43
2.5	-	$x(138,140)$	19.95	10.35	6.96
2.5	RT	$x(139,203)$	0.76	1.02	1.00
2.5	-	$x(139,104)$	19.73	10.93	7.19
3.0	RT	$x(103,104)$	6.15	3.65	2.30
3.0	-	$x(103,108)$	2.09	15.79	8.06
3.0	RT	$x(138,108)$	1.08	1.08	1.07
3.0	-	$x(138,140)$	20.69	10.12	6.73
3.0	RT	$x(139,203)$	0.79	0.79	0.78
3.0	-	$x(139,104)$	20.5	10.13	6.85

Table 2: Delays in all queues at intersection 103. RT means right turn.

<i>C</i>	Delay w RT FT	Delay w RT MP4	Delay w RT MP6	Delay wo RT FT	Delay wo RT MP4	Delay wo RT MP6
1.0	9.9	7.6	5.4	15.7	12.0	7.9
1.5	7.3	7.1	4.5	12.7	11.7	6.9
2.0	7.9	7.1	4.4	13.5	12.0	7.1
2.5	8.2	7.0	4.3	14.0	12.1	7.0
3	8.6	6.9	4.3	14.4	12	7.2

Table 3: Average delay at intersection 103. RT means right turn.

speed up,  $g = 1$ , being the base case. If we take MP4 as the base case, then MP6 corresponds to  $g = 1.5$  (six vs four phase switches per cycle). So according to (12) and (17) the mean queue length under MP4 should be 1.5 times the mean queue length under MP6, for every demand. Going back to Table 1, we see that the ratios of the sum of queue lengths under MP4 to the length under MP are: 1.45, 1.46, 1.5, 1.6, and 1.6 for  $C = 1, 1.5, 2.0, 2.5$  and  $3.0$ . A similar prediction is upheld in Table 3: the ratio of delays under MP4 and MP6 at queues in intersection 103 lie within a narrow band around 1.7 which can be compared to a switching speed up of  $g = 1.5$ .

## 5 Conclusion

Intersections are the bottlenecks of urban roads, since their capacity is about one quarter of the maximum vehicle flow that can be accommodated by the approaches to the intersection. This bottleneck capacity can be increased by a factor of two to three if vehicles are organized to cross the intersection in platoons with 0.75s headway at 45 mph or 0.7s headway at 30 mph to achieve a saturation flow rate of 4800 vph per lane. Vehicles crossing an intersection in a platoon must have at a minimum the following capabilities. When the signal is actuated (light turns green) all queued vehicles must move together. This requires a common ‘start’ signal from the intersection controller or the first vehicle at the beginning of green, and a constant time-gap car-following control strategy. In order to move together, the platoon control must ensure ‘string stability’ (Swaroop and Hedrick (1996)). It is also necessary for newly arriving vehicles to be able to join the platoon as it is moving. A ‘stop’ signal indicating end of green should terminate the platoon and prevent any vehicle from entering the intersection.

Over the past five years, several platooning experiments have been reported in which factory-equipped ACC vehicles have been augmented by V2V communication capability. The augmented vehicles can operate in CACC mode. For example, Ploeg et al. (2011) report a 6-vehicle CACC platoon, with a 0.5s headway; and Milanes et al. (2014) describe a 4-vehicle CACC platoon, with a 0.8s headway, capable of cut-in, cut-out and other maneuvers. Thus the minimum requirements for platooning can be met. All that the driver needs to do is to engage the CACC mode upon approaching the intersection and disengage it after crossing the intersection. There are additional questions that need to be addressed. Should the intersection provide a target speed? Should it suggest a minimum or maximum platoon size? Should vehicles continue in platoon formation after crossing the intersection?

The paper explores the urban mobility benefits of larger saturation flow rates using queuing analysis and a simulation case study. The study reaches the following conclusions. If the saturation flow rate is increased by a factor  $C$ , the network can support an increase in demand by the same factor  $C$ , with no increase in queuing delay or travel time, and using the same signal control. However, the queues will also grow by the same factor  $C$ , so if this leads to a saturation of the links, the improvement in throughput will be sub-linear in  $C$ . On the other hand, if the cycle time is reduced, the queues will also be reduced, and this may restore the linear growth in demand.

These dramatic conclusions indicate a pure productivity increase of the urban infrastructure by an unprecedented 200 to 300 percent using connected vehicle technology. The productivity increase can be shared between increased demand and a reduction in queuing delay by reducing the cycle time.

## References

- T-C. Au, S. Zhang, and P. Stone. Autonomous intersection management for semi-autonomous vehicles. In *Handbook of Transportation*. Routledge, Taylor & Francis Group, 2015.
- D. Bezzina and J. Sayer. Safety pilot model deployment: Test conductor team report. Report No. DOT HS 812 171, Washington, DC: National Highway Traffic Safety Administration., June 2015.
- C.M. Day, D.M. Bullock, H. Li, S.M. Remias, A.M. Hainen, A.L. Stevens, J.R. Sturdevant, and T.M. Brennan. Performance measures for traffic signal systems: An outcome-oriented approach. Technical report, Purdue University, Lafayette, IN, 2014. doi: 10.5703/1288284315333.
- FHWA. Traffic Control Systems Handbook. <http://ops.fhwa.dot.gov/publications/fhwahop06006/index.htm>.
- A. Gandhi, M. Harchol-Balter, S. Doroudi, and A. Scheller-Wolf. Exact analysis of the m/m/k/setup class of Markov chains via recursive renewal reward. *Sigmetrics'13*, June 17-21 2013.
- M. R. Hafner, D. Cunningham, L. Caminiti, and D. Del Vecchio. Cooperative collision avoidance at intersections: Algorithms and experiments. *IEEE Trans. Intelligent Transportation Systems*, 14(3):1162–1175, Sept 2013.
- J. Harding, G.R. Powell, R. Yoon, J. Fikentscher, C. Doyle, D. Sade, M. Lukuc, M. Simons, and J. Wang. Vehicle-to-vehicle communications: Readiness of V2V technology for application. Report No. DOT HS 812 014, Washington, DC: National Highway Traffic Safety Administration., August 2014.
- R. Kianfar, B. Augusto, A. Ebadighajari, U. Hakeem, J. Nilsson, A. Raza, R. Tabar, V. N. C. Englund, P. Falcone, S. Papanastasiou, L. Svensson, and H. Wymeersch. Design and experimental validation of a cooperative driving system in the grand cooperative driving challenge. *IEEE Trans. Intelligent Transportation Systems*, 13(3):994–1007, 2012.
- G. Latouche and V. Ramaswami. *Introduction to Matrix Analytic Methods in Stochastic Modeling*. ASA-SIAM, Philadelphia, 1999.
- V. Milanés, S. E. Shladover, J. Spring, Christopher Nowakowski, H. Kawazoe, and M. Nakamura. Cooperative adaptive cruise control in real traffic situations. *IEEE Trans. Intelligent Transportation Systems*, 15(1):296–305, Feb 2014.
- A. Muralidharan, R. Pedarsani, and P. Varaiya. Analysis of fixed-time control. *Transportation Research Part B: Methodological*, 73:81–90, March 2015.
- NAHSRC. Automated Highway Demo 97. [https://www.youtube.com/watch?v=C9G6JRUmg\\_A](https://www.youtube.com/watch?v=C9G6JRUmg_A).
- J. Ploeg, B. T. M. Scheepers, E. van Nunen, N. van de Wouw, and H. Nijmeijer. Design and experimental evaluation of cooperative adaptive cruise control. *Proc. 14th ITSC IEEE Conf*, pages 260–265, 2011.
- S.E. Shladover. Why automated vehicles need to be connected vehicles, 2013. [http://www.ewh.ieee.org/tc/its/VNC13/IEEE\\_VNC\\_BostonKeynote\\_Shladover.pdf](http://www.ewh.ieee.org/tc/its/VNC13/IEEE_VNC_BostonKeynote_Shladover.pdf).
- D. Swaroop and J. Hedrick. String stability of interconnected systems. *IEEE Trans. Autom. Control*, 41(3):349–357, March 1996.



F. Y. Tascikaraoglu, J. Lioris, A. Muralidharan, M. Gouy, and P. Varaiya. Pointq model of an arterial network: calibration and experiments, July 2015. <http://arxiv.org/abs/1507.08082>.

Transportation Research Board. *Highway Capacity Manual*. Washington DC, 2010.

USDOT. Connected Vehicle Research in the United States, 2015. [http://www.its.dot.gov/connected\\_vehicle/connected\\_vehicle\\_research.htm](http://www.its.dot.gov/connected_vehicle/connected_vehicle_research.htm).

W. K. Wolterink, G. Heijenk, and G. Karagiannis. Automated merging in a cooperative adaptive cruise control (CACC) system. <http://doc.utwente.nl/77622/1/KleinWolterink11automated.pdf>.

J. Yoshida. Vehicle-to-Vehicle: 7 Things to Know About Uncle Sam's Plan. EE Times, 8/22/2014, 2014.